

Trajectory and Force Generation with Multi-constraints for Robotic Belt Grinding

Yangyang Mao, Huan Zhao^(✉), Xin Zhao, and Han Ding

State Key Laboratory of Digital Manufacturing Equipment and Technology,
Huazhong University of Science and Technology, Wuhan 430074, Hubei,
People's Republic of China
huanzhao@hust.edu.cn

Abstract. In the robotic belt grinding process, the parameters such as robot feedrate and contact force play important roles on the material removal. In order to minimize the machining time and achieve high accuracy, a scheduling method of trajectory and force is proposed to maximize the robot feedrate. First, an optimization model with the constraints of joints speed, acceleration and robot feedrate, acceleration of robotic belt grinding is presented. Then, the feedrate scheduling problem is transferred to a linear programming problem, which can be solved efficiently. The contact force is also scheduled based on an empirical formula of grinding mechanism after solving the optimal feedrate. Finally, the simulation and experiment show the method can effectively achieve trajectory and force generation for robotic belt grinding with high efficiency and accuracy.

Keywords: Trajectory generation · Force generation · Robotic belt grinding

1 Introduction

To date, robotic belt grinding has been extensively applied to achieve high material removal rate in aeronautics industry, which can relieve hand grinders from their noisy work environment as well as for improving machining accuracy and product consistency [1]. Therefore, it is necessary to control the material removal process during belt grinding processes, especially in the complex workpiece surface machining (e.g., surfaces of turbine blades) [2]. However, the material removal is related to a variety of factors. It is revealed that the robot feedrate and the workpiece-wheel contact force are the two key process parameters as shown in Fig. 1. Therefore, the key problems of controlling the material removal amount of robotic belt grinding are to schedule the robot feedrate and contact force.

Song et al. [3] proposed the optimization model which is the minimum changes in robot feedrate and contact force at the next point to reduce the influence of the transition process caused by the control adjustment, through the predicted removal error at a grinding point. The method could effectively track the desired material removal, but the robot could not precisely track the desired parameter trajectories planned offline.

Wu [4] employed a conservative strategy which could be used to solve the optimization problem by setting an objective function defined to minimize the difference between the actual material removal and the expected material removal. The robot feedrate and contact force to reach/pass the target were taken into consideration in the strategy. The method was the most direct and effective for the grinding of the complex geometries, but it required real-time measuring the amount of the complex blades so that the process was time-consuming and the production efficiency was not high. Ren and Kuhlenkötter [5] introduced a local process model where the force distribution in the contact area was determined via a finite element model constructed using a set of geometry and elasticity information on the intersection between the grinding belt and the workpiece. It is no doubt that this method increases the computational burden. Zhao et al. [6] developed an adaptive feedrate optimization model with the constraints of chord error, maximum feedrate, acceleration and jerk to minimize the machining time, but this method was only applicable to five-axis machining. Song et al. [7] presented a planning method for the control parameters of the grinding robot based on an adaptive modeling using the cooperative particle swarm optimization. It aimed to smooth the trajectories of the control parameters of the robot and shorten the response time in the transition process. However, the optimization goal was too complex which increased the computational load.

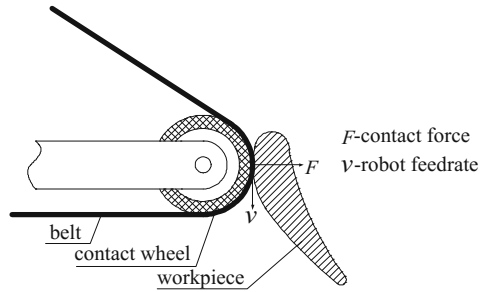


Fig. 1. Illustration of the robot feedrate and contact force.

This paper presents a method of trajectory and force generation which aims to minimize the machining time. First, the optimization model simultaneously constrains the joints speed, acceleration and robot feedrate, acceleration. And the model is transferred to a linear optimization problem. Then, after solving the optimal robot feedrate, the contact force could be calculated based on an empirical approximate formula of grinding mechanism. Compared with the existing methods, the proposed method is efficient and can be applied in practical applications.

The rest of this paper is organized as follows. The tool path fitting into the B-spline with respect to parameter u is introduced in Sect. 2. Section 3 presents the scheduling algorithm with multi-constraints in detail. Simulation and experiment are provided in Sect. 4, followed by the conclusion in Sect. 5.

2 Tool Path Fitting into the B-Spline

The tool path of robotic belt grinding is commonly given by a sequence of discrete cut location (CL) points, which are generated according to chord error and scallop height [8, 9]. Each CL point consists of tool center position and orientation. The challenge in converting tool paths into axis motions is to command the tool to move at the specified feedrate. Because it is impractical to specify the axis positions at the motion controller loop closing frequency, interpolatory splines are used [10]. In addition, the tool tip and orientation locations are first fitted to splines independently to achieve geometric continuity while decoupling the relative changes in position and orientation of the cutter along the curved path [11]. Therefore, the tool center position and orientation of the spline path are defined as a function of parameter u .

$$\begin{cases} \mathbf{p}(u) = \sum_{i=0}^n N_{i,k}(u) \omega_i \mathbf{p}_i / \sum_{i=0}^n N_{i,k}(u) \omega_i \\ \mathbf{o}(u) = \sum_{i=0}^n N_{i,k}(u) \omega_i \mathbf{o}_i / \sum_{i=0}^n N_{i,k}(u) \omega_i \end{cases} \quad (1)$$

where \mathbf{p}_i and \mathbf{o}_i are control points, which are obtained by the post-processing of the tool path. $\mathbf{p}(u) = [p_x(u), p_y(u), p_z(u)]$ describes the wheel center curve. $\mathbf{o}(u) = [o_x(u), o_y(u), o_z(u)]$ represents the orientation axis curve, which are calculated by the control points. And if the orientation of the tool is defined by a unit vector, the orientation spline must lie on the surface of the unit sphere. ω_i is the weight coefficient. $N_{i,k}(u)$ is the k th B-spline basis function of k -degree [12], and is defined as

$$\begin{aligned} N_{i,0} &= \begin{cases} 0, & u_i \leq u \leq u_{i+1} \\ 1, & \text{otherwise} \end{cases} \\ N_{i,k}(u) &= \frac{u - u_i}{u_{i+k} - u_i} N_{i,k-1}(u) + \frac{u_{i+k+1} - u}{u_{i+k+1} - u_{i+1}} N_{i+1,k-1}(u) \end{aligned} \quad (2)$$

where $U = [u_0, u_1, \dots, u_m]$ is the knot vector. And $\mathbf{x}(u) = [\mathbf{p}(u), \mathbf{o}(u)]^T$ can denote the pose of the robot.

3 Scheduling Algorithm for Trajectory and Force

3.1 Optimization Goal

The purpose of the scheduling method aims to minimize the machining time while taking joint speed, acceleration and robot feedrate, acceleration into consideration. Since $dt = |\mathbf{p}'|du/v(u)$, the optimization goal could be designed as follows:

$$\min \int_0^1 |\mathbf{p}'| du / v(u) \quad (3)$$

Because of solving the Eq. (3) is time-consuming, the optimization goal could be transferred to maximize the feedrate by discretizing the tool path with equal interval of parameter u . At last, the optimization goal could be rewritten as below:

$$\max \sum_{i=0}^n \left(\frac{v(u_i)}{|\mathbf{p}'(u_i)|} \right)^2 \quad (4)$$

3.2 Trajectory Generation

3.2.1 Joint Constraints

In the robotic machining process, joint constraints must be taken into consideration firstly. Therefore, the speed and the acceleration of six joints must not exceed their limits. Because the speed and acceleration of the six joints are done by interpolation of the joint values, they are taken into consideration in joint space. According to the conditions, the constraints could be evaluated as

$$\dot{\theta}_{\min} \leq \dot{\theta}(u) \leq \dot{\theta}_{\max} \quad (5)$$

$$\ddot{\theta}_{\min} \leq \ddot{\theta}(u) \leq \ddot{\theta}_{\max} \quad (6)$$

where $\dot{\theta}(u) = [\dot{\theta}_1(u), \dot{\theta}_2(u), \dot{\theta}_3(u), \dot{\theta}_4(u), \dot{\theta}_5(u), \dot{\theta}_6(u)]^T$ is the speed of six joints of the robot. And $\ddot{\theta}(u) = [\ddot{\theta}_1(u), \ddot{\theta}_2(u), \ddot{\theta}_3(u), \ddot{\theta}_4(u), \ddot{\theta}_5(u), \ddot{\theta}_6(u)]^T$ is the acceleration of six joints. $\dot{\theta}_{\min}(\ddot{\theta}_{\min})$ and $\dot{\theta}_{\max}(\ddot{\theta}_{\max})$ are the minimum and maximum values of the speed (acceleration) of six joints, respectively. And the limits of the speed and acceleration, which we can look up, are usually provided by the robot manufacturer.

Since $\dot{\mathbf{x}}(u) = J\dot{\theta}(u)$, where $\dot{\mathbf{x}}(u)$ denotes the derivatives of $\mathbf{x}(u)$ with time, J is the jacobian matrix, Eqs. (5) and (6) can be described as

$$\dot{\theta}(u)^T = \frac{J^{-1}\mathbf{x}'(u)^T}{|\mathbf{p}'(u)|} v(u) \quad (7)$$

$$\ddot{\theta}(u)^T = J^{-1} \left[\left(\frac{1}{|\mathbf{p}'(u)|^2} \mathbf{x}''(u)^T - \frac{\mathbf{p}'(u) \cdot \mathbf{p}''(u)}{|\mathbf{p}'(u)|^2} \mathbf{x}'(u)^T \right) v^2(u) - J\dot{\theta}(u) \right] \quad (8)$$

$\mathbf{x}'(u)$ and $\mathbf{x}''(u)$ are the derivatives of $\mathbf{x}(u)$ with parameter u . $\mathbf{p}'(u)$ and $\mathbf{p}''(u)$ are the derivatives of $\mathbf{p}(u)$ with parameter u .

3.2.2 Grinding Process Constraints

In the process of robotic belt grinding, the feedrate and acceleration of end-effector could be related to the speed and acceleration of the six joints through the jacobian. However, for the sake of convenience, the feedrate and acceleration of the end effector could be obtained by interpolation of the positions in base frame, which are collected in

Cartesian space. In addition, the limits of the feedrate and acceleration of the end effector are determined by the machining process experiences.

v_{\lim} is the maximum robot feedrate, so the feedrate under this constraints is as following:

$$0 \leq v(u_i) \leq v_{\lim} \quad (9)$$

The acceleration of robotic end-effector is obtained by the difference of the feedrate, which could be written as:

$$a(u_i) = \frac{v(u_{i+1}) - v(u_i)}{\Delta t} = \frac{v(u_{i+1})^2 - v(u_i)^2}{2|\mathbf{p}'(u_i)|\Delta u} \quad (10)$$

where Δu is the interval of parameter u . When the maximum acceleration a_{\lim} is given, the under constraints can be obtained.

$$-a_{\lim} \leq \frac{v(u_{i+1})^2 - v(u_i)^2}{2|\mathbf{p}'(u_i)|\Delta u} \leq a_{\lim} \quad (11)$$

3.2.3 Detailed Algorithm

Because Eqs. (5), (6), (9) and (11) have established the linear constraints with respecting joint constraints and process constraints, the detailed algorithm is summarized by using the equations above.

Assuming that the parameter u is sampled with equal interval and using the Eqs. (7) and (9), the robot feedrate could be calculated as following:

$$v_r(u_i) = \min \left\{ \frac{|J\dot{\theta}(u_i)^T|}{|\mathbf{x}'(u_i)^T|} |\mathbf{p}'(u_i)|, v_{\lim} \right\} \quad (12)$$

In the machining process, the robot feedrate $v(u_i)$ should be less than or equal to $v_r(u_i)$. At the beginning and the end of the path, the feedrates of the first and end point should be set to equal to a constant value, that is $v(0) = v_{first}$, $v(1) = v_{end}$. Using $v_i^2 (i = 0, \dots, n)$ as the design vector, the optimization model of robot feedrate is arranged as

$$\begin{aligned} & \max \sum_{i=0}^n \frac{v_i^2}{|\mathbf{p}'(u_i)|^2} \\ & s. t. \\ & \begin{cases} v_0 = v_{first}, v_n = v_{end} \\ 0 \leq v_i^2 \leq v_r^2(u_i) \\ -a_{\lim} \leq \frac{v(u_{i+1})^2 - v(u_i)^2}{2|\mathbf{p}'(u_i)|\Delta u} \leq a_{\lim} \\ \ddot{\theta}(u)^T = J^{-1} \left[\left(\frac{1}{|\mathbf{p}'(u)|^2} \mathbf{x}''(u)^T - \frac{\mathbf{p}'(u)\mathbf{p}''(u)}{|\mathbf{p}'(u)|^2} \mathbf{x}'(u)^T \right) v^2(u) - J\dot{\theta}(u) \right] \end{cases} \end{aligned} \quad (13)$$

Note that Eq. (13) is a linear programming problem, so the scheduling feedrate could be solved effectively and easily.

3.3 Force Generation

Using the grinding mechanism, some empirical equations for modeling process are available and have been applied in practical systems [13]. For grinding a workpiece with a complex surface, an empirical approximate formula is given in [14] and [15] as

$$r = K \frac{(v_b)^\alpha}{(v)^\beta} (F)^\gamma \quad (14)$$

where r denotes the amount of the material removal, K is a constant that describes the grinding factors. v_b is the grinding belt velocity and usually could be set to a constant value. v is the robot feedrate and F is the contact force. α, β, γ are constant coefficients.

After solving the optimal robot feedrate from Eq. (13), the contact force could be calculated from Eq. (14) when r, K and v_b are known. Naturally, a maximum value of the contact force F_{lim} should be set because too high contact force would cause too much heat between the belt and the workpiece, which would burn the workpiece. At the beginning and the end of the path, the forces of the first and end point should be set to equal to a constant value, that is $F(0) = F_{first}, F(1) = F_{end}$. When the calculated contact force exceed the maximum value F_{lim} , the robot feedrate should be scheduled again from Eq. (13). While the robot feedrate and contact force could satisfy the all requirements finally, a cubic B-spline is used to fit the robot feedrate and contact force with respect to parameter u . Besides, after the contact force of robotic belt grinding is calculated and optimized, the position-based impedance control could be used for robotic time-varying force tracking, which would achieve the accurate robotic belt grinding force control [16, 17].

4 Simulation and Experiment

The proposed scheduling method is applied to a length of tool path based on robotic belt grinding as shown Fig. 2(a). And the tool path is described in the workpiece coordinate system. The parameters used in the scheduling method are list in Table 1. Figure 2(b) denotes the desire material removal. The robot feedrate and contact force could be scheduled according to the scheduling algorithm as shown Fig. 2(c). The acceleration of robot end-effector is described as shown Fig. 2(d). The speed and acceleration of six joints are given in Fig. 2(e–f).

We may know the scheduling feedrate and force are continuous from Fig. 1. The feedrate and acceleration of each joint, the robot feedrate, acceleration and contact force do not exceed their setting value, thus proving the effectiveness of the scheduling algorithm.

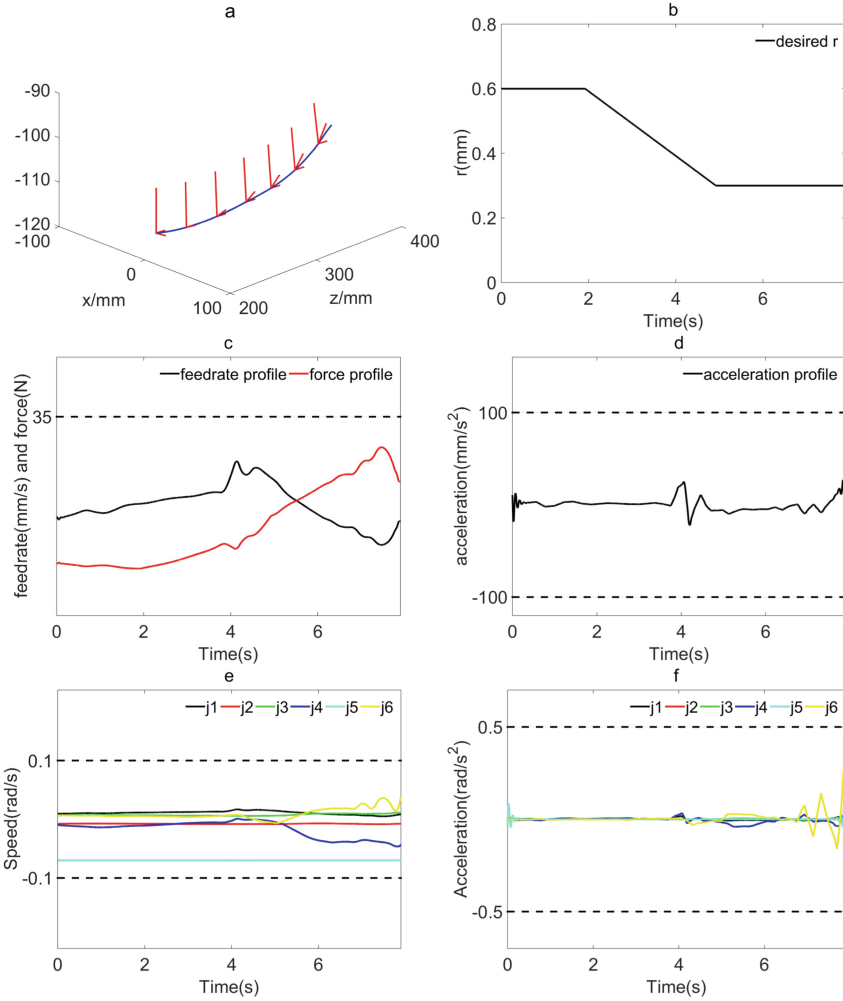
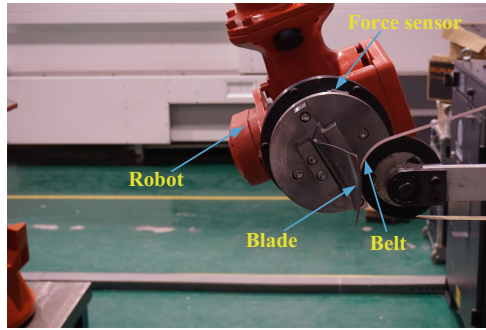


Fig. 2. Results of the scheduling method. (a) Tool path of robotic belt grinding. (b) Desired material removal. (c) Robot feedrate and contact force profile. (d) Robot acceleration profile. (e) The speed of six joints. (f) The acceleration of six joints.

The experiment has been conducted in the robotic belt grinding system to validate the proposed scheduling algorithm as shown Fig. 3. The robot is COMAU-Smart-NJ220 controlled by the C5G-Open which can acquire the robot feedrate. The force sensor is ATI omega160 which can measure the contact force accurately. The workpiece for the grinding experiments is a real airfoil blade made of titanium alloy with a free-form surface. The type of belt is GXK-51 P180 dedicated to grinding precise parts.

Table 1. Scheduling parameters for simulation

Parameters	Value
Parameter interval Δu	0.001
Interpolation period $T(s)$	0.001
Maximum feedrate $v_{lim}(mm/s)$	35
Maximum force $F_{lim}(N)$	35
Feedrate of first point $v_{first}(mm/s)$	17.4
Feedrate of end point $v_{end}(mm/s)$	15.6
Force of first point $F_{first}(N)$	9.1
Force of end point $F_{end}(N)$	24.8
Maximum acceleration $a_{lim}(mm/s^2)$	100
Minimum joints speed $\dot{\theta}_{min}(rad/s)$	$[-0.1]_{1 \times 6}^T$
Maximum joints speed $\dot{\theta}_{max}(rad/s)$	$[0.1]_{1 \times 6}^T$
Minimum joints acceleration $\ddot{\theta}_{min}(rad/s^2)$	$[-1]_{1 \times 6}^T$
Maximum joints acceleration $\ddot{\theta}_{max}(rad/s^2)$	$[1]_{1 \times 6}^T$
Belt velocity $v_b(mm/s)$	25
Grinding factors constant K	1277.6
Constant coefficient α	-1.1107
Constant coefficient β	-0.5931
Constant coefficient γ	-0.7563

**Fig. 3.** Robotic belt grinding system.

The results of the experiment could be seen in Fig. 4. From the Fig. 4, we can know that the actual material removal is very close to the desired material removal. And the relative error is below 15%. This proves a higher grinding removal precision is obtained and the robot tracks the desired material removal more effectively after the optimal generation of the robot velocity and contact force.

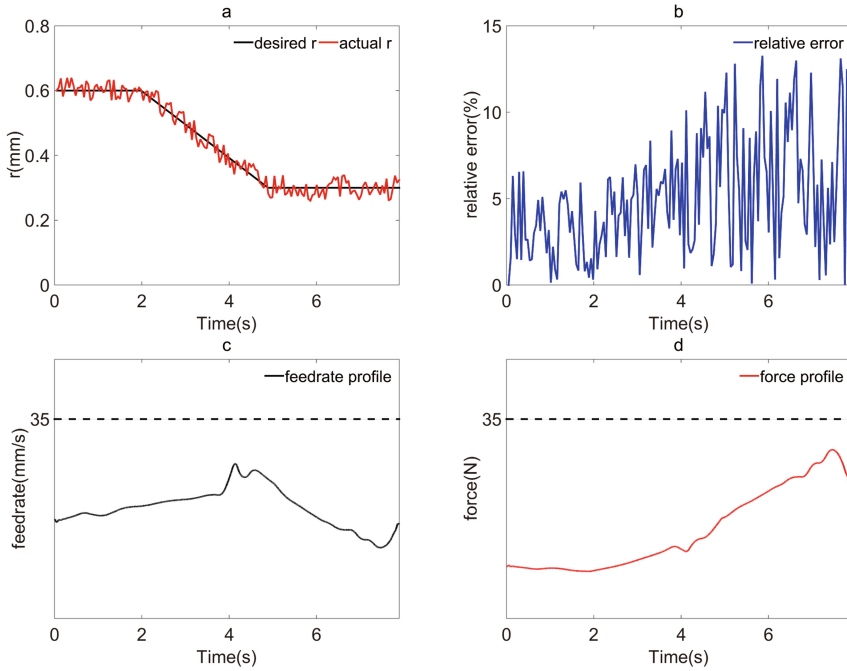


Fig. 4. Results of the experiment. (a) Desired material removal and actual one. (b) Relative error of the material removal. (c) Robot feedrate profile. (d) Contact force profile.

5 Conclusion

The trajectory and force for robotic belt grinding are scheduled effectively in this paper. First, the optimization method with respect to the constraints of joints speed, acceleration and robot feedrate, acceleration is proposed to maximize the feedrate in order to achieve high machining efficiency. Then, the model is transferred to a linear optimization problem which can be solved efficiently. After solving the optimal robot feedrate, the contact force could be calculated based on an empirical approximate formula of grinding mechanism. Finally, the simulation and experiment are conducted, which show the method can excellently achieve trajectory and force generation for robotic belt grinding with high efficiency and accuracy.

Acknowledgements. This work was supported by the National Natural Science Foundation of China under Grant Nos. 51535004, 51323009, 51375196 and 51405175.

References

1. Yun, H., Zhi, H.: Modern belt grinding technology and engineering applications (2009)
2. Wang, Y., Hou, B., Wang, F., et al.: A controllable material removal strategy considering force-geometry model of belt grinding processes. *Int. J. Adv. Manufact. Technol.*, 1–11 (2016)

3. Song, Y., Yang, H., Lv, H.: Intelligent control for a robot belt grinding system. *IEEE Trans. Control Syst. Technol.* **21**(3), 716–724 (2013)
4. Wu, S.: Robotic conformance grinding modeling, control and optimization. Diss. Theses - Gradworks (4), 337 (2012)
5. Ren, X., Kuhlenkötter, B.: Real-time simulation and visualization of robotic belt grinding processes. *Int. J. Adv. Manufact. Technol.* **35**(11), 1090–1099 (2008)
6. Zhao, X., Zhao, H., Yang, J., Ding, H.: An adaptive feedrate scheduling method with multi-constraints for five-axis machine tools. In: Liu, H., Kubota, N., Zhu, X., Dillmann, R., Zhou, D. (eds.) *ICIRA 2015. LNCS*, vol. 9245, pp. 553–564. Springer, Cham (2015). doi:[10.1007/978-3-319-22876-1_48](https://doi.org/10.1007/978-3-319-22876-1_48)
7. Song, Y., Liang, W., Yang, Y.: A method for grinding removal control of a robot belt grinding system. *J. Intell. Manufact.* **23**(5), 1903–1913 (2012)
8. Choi, Y.K., Banerjee, A., Lee, J.W.: Tool path generation for free form surfaces using Bézier curves/surfaces. *Comput. Ind. Eng.* **52**(4), 486–501 (2007)
9. Choquet-Bruhat, Y.: Tool path generation and tolerance analysis for free-form surfaces. *Int. J. Mach. Tools Manufact.* **47**(3–4), 689–696 (2007)
10. Fleisig, R.V., Spence, A.D.: A constant feed and reduced angular acceleration interpolation algorithm for multi-axis machining. *Comput.-Aided Des.* **33**(1), 1–15 (2001)
11. Yuen, A., Zhang, K., Altintas, Y.: Smooth trajectory generation for five-axis machine tools. *Int. J. Mach. Tools Manufact.* **71**(8), 11–19 (2013)
12. Piegl, L., Tiller, W.: *The NURBS Book*. Springer, Heidelberg (1997). doi:[10.1007/978-3-642-59223-2](https://doi.org/10.1007/978-3-642-59223-2)
13. Wang, J., Sun, Y., Gan, Z., Kazerounian, K.: Process modeling of flexible robotic grinding. In: *Proceedings of the International Conference Control, Automation System* (2003)
14. Hammann, G.: Modellierung des abtragaverhaltens elastischer robotergeführter schleifwerkzeuge. Ph.D. Dissertation, Institute for Control Engineering of Machine Tools and Manufacturing Units, University of Stuttgart, Stuttgart, Germany (1998)
15. Schueppstuhl, T.: Beitrag zum bandschleifen komplexer freiformgeometrien mit dem industriroboter. Ph.D. Dissertation, Mechanical Engineering Department, Technical University of Dortmund, Dortmund, Germany (2003)
16. Xu, W., Cai, C., Yin, M., et al.: Time-varying force tracking in impedance control a case study for automatic cell manipulation. In: *IEEE International Conference on Control and Automation*. pp. 344–349. IEEE (2013)
17. Xie, Y., Sun, D., Liu, C., et al.: An adaptive impedance force control approach for robotic cell microinjection. In: *IEEE/RSJ International Conference on Intelligent Robots and Systems*, pp. 907–912. IEEE (2008)

Intelligent Robotics and Applications

10th International Conference, ICIRA 2017, Wuhan,
China, August 16–18, 2017, Proceedings, Part II

Huang, Y.; Wu, H.; Liu, H.; Yin, Z. (Eds.)

2017, XIX, 907 p. 626 illus., Softcover

ISBN: 978-3-319-65291-7